Mechanisms of Ageing and Development 198 (2021) 111547

Contents lists available at ScienceDirect

Mechanisms of Ageing and Development

journal homepage: www.elsevier.com/locate/mechagedev

MicroRNA profiles of human peripheral arteries and abdominal aorta in normal conditions: MicroRNAs-27a-5p, -139-5p and -155-5p emerge and in atheroma too

Salvatore Collura [a], Carmen Ciavarella [a], Cristina Morsiani [a], Ilenia Motta [a], Sabrina Valente [a], Enrico Gallitto [b], Mohammad Abualhin [b], Rodolfo Pini [b], Francesco Vasuri [c], Claudio Franceschi [a,d], Miriam Capri [a,e,*,1], Mauro Gargiulo [a,b,1], Gianandrea Pasquinelli [a,f,1]

[a] DIMES-Department of Experimental, Diagnostic and Specialty Medicine, University of Bologna, Bologna, Italy
[b] Unit of Vascular Surgery, IRCCS, Policlinico S. Orsola Hospital, Bologna, Italy
[c] Unit of Pathology, IRCCS, Policlinico S. Orsola Hospital, Bologna, Italy
[d] Department of Applied Mathematics of the Institute of ITMM, National Research Lobachevsky State University of Nizhny Novgorod, Russian Federation
[e] Interdepartmental Center - Alma Mater Research Institute on Global Challenges and Climate Change - University of Bologna, Bologna, Italy
[f] Subcellular Nephro-Vascular Diagnostic Program, Pathology Unit, IRCCS, Policlinico S. Orsola Hospital, Bologna, Italy

ARTICLE INFO

Keywords:
Normal arteries
Atherosclerosis
Biomarkers
Aging
microRNAs

ABSTRACT

Atherosclerosis may starts early in life and each artery has peculiar characteristics likely affecting atherogenesis. The primary objective of the work was to underpin the microRNA (miR)-profiling differences in human normal femoral, abdominal aortic, and carotid arteries. The secondary aim was to investigate if those identified miRs, differently expressed in normal conditions, may also have a role in atherosclerotic arteries at adult ages. MiR-profiles were performed on normal tissues, revealing that aorta and carotid arteries are more similar than femoral arteries. MiRs emerging from profiling comparisons, *i.e.*, miR-155-5p, -27a-5p, and -139-5p, were subjected to validation by RT-qPCR in normal arteries and also in pathological/atheroma counterparts, considering all the available 20 artery specimens. The three miRs were confirmed to be differentially expressed in normal femoral *vs* aorta/carotid arteries. Differential expression of those miRs was also observed in atherosclerotic arteries, together with some miR-target proteins, such as vimentin, CD44, E-cadherin and an additional marker SLUG. The different expression of miRs and targets/markers suggests that aorta/carotid and femoral arteries differently activate molecular drivers of pathological condition, thus conditioning the morphology of atheroma in adult life and likely suggesting the future use of artery-specific treatment to counteract atherosclerosis.

1. Introduction

Atherosclerosis has a long, slow asymptomatic phase, starting early in life, several years before the onset of clinical signs (Libby et al., 2019; Rea et al., 2018) and in many patients becoming manifest at a relatively advanced age. Thus, the biological age could be considered the most important atherosclerosis risk factor, associating with artery-specific molecular and physiological characteristics which interact with many variables and may have a role in atheroma development, such as gender, genetic makeup, aging process, regenerative intrinsic abilities, lifestyles, and socioeconomic status (Collura et al., 2020; Sigala et al., 2018).

The role of arteriogenesis remains a relevant starting point to understand morphological and molecular differences of atherosclerosis among various arteries. Arteriogenesis starts during embryonic vascular development leading to arterial specifications, including morphology, structure/topology and physiology, for each arterial district of the human body. In particular, fate mapping studies have demonstrated highly heterogeneous origins of smooth muscle cells (SMCs) and other vascular wall resident cells. Accordingly, in the pharyngeal arch arteries as well as their derivatives including the carotid arteries, SMCs arise from the neural crest. The aorta is composed of regions originating from two distinct germ layers; the aortic arch region comes from the ectoderm

* Corresponding author at: Via San Giacomo, 12, DIMES- Department of Experimental, Diagnostic and Specialty Medicine, Alma Mater Studiorum, University of Bologna, 40126, Bologna, Italy.
[1] Co-senior Authorship.

https://doi.org/10.1016/j.mad.2021.111547
Received 30 April 2021; Received in revised form 12 July 2021; Accepted 22 July 2021
Available online 28 July 2021

and is populated by SMC (Jiang et al., 2000); the ascending and descending abdominal aorta are instead of mesodermal origin (Pouget et al., 2006; Verzi et al., 2005; Wasteson et al., 2008; Wiegreffe et al., 2009).

As far as atheroma is concerned, it retains its characteristic in atheroma-prone abdominal aorta when transplanted to any region of the aorta using aortic homograft transplantations in animal model; in reciprocal experiments, the low atheroma-prone thoracic aorta does not develop atherosclerotic lesions when placed in high-risk regions (Haimovici et al., 1959, 1958; Haimovici and Maier, 1964).

Significant arterial heterogeneity among different arterial beds seems to be observed as well as different kinetics of atheroma progression exist according to the arterial region and cellular architecture. Carotid and femoral plaques are characterized by different histotypes; the prevalence of fibro-lipidic, inflammatory plaques in the carotid district and the prevalence of fibro-calcific plaque in the femoral bed have been found (Dalager et al., 2007; Herisson et al., 2011; Vasuri et al., 2016).

However, the literature on the differences among healthy human arteries and their different atheroma onset and characteristics is scanty (Vasuri et al., 2020, 2016). Those differences could origin through genetic-epigenetic interactions. In particular, microRNAs (miRs) as epigenetic regulators in arteries and evaluable biomarkers in pathological conditions, have been studying for many years (Goossens et al., 2019; Tzoulaki et al., 2019). Nevertheless, the difference in terms of miR-profiles among healthy arteries has not yet been established.

The primary objective of the present work was to underpin the miR-profiling differences in human femoral, abdominal aortic, and carotid arteries aiming at the identification of miRs likely involved in epigenetics changes of these arteries in normal conditions. The secondary aim is to investigate if those identified miRs, differentially expressed in normal conditions, may also have a role in atherosclerotic arteries in adult patients. The selection of the above-mentioned arteries was motivated by their embryological origin, histopathological and genetic-molecular distinctive heterogeneity.

2. Materials and methods

2.1. Biopsies

Artery biopsies were obtained by the Pathology ward at S.Orsola Hospital (Bologna, Italy), as retrospective study with the approval of the local ethical committee (88/2019/Sper/AOUBo). Ten healthy arteries acquired from organ donors (5 females, 5 males, mean age 35 ± 8) and 10 atherosclerotic plaque biopsies, obtained from patients (3 females, 7 males, mean age 56 ± 8) with endarterectomy due to hemodynamically significant atherosclerosis or open surgery, represent the population sample of the study. Specifically, the number of carotid, femoral and abdominal aorta artery biopsies are described in Table 1.

All patients were anonymized and data were treated according to the ethical guidelines of the 1975 Declaration of Helsinki and following revisions including the most recent privacy GDPR laws (EU, 2016/679).

2.2. Biopsy processing and histology

Biopsies were formalin fixed, paraffin embedded (FFPE) and routinely processed. Two-μm-thick sections were cut and stained with Haematoxylin-Eosin.

2.3. RNA extraction from FFPE tissue

Total RNA was extracted from FFPE sections. Briefly, 4 slices of 20 μm thickness from each selected biopsy block were deparaffinized (~20 min) and digested with protease (overnight at 50 °C and 15 min at 80 °C). RNA extraction was obtained using a commercial kit (RecoverAll™ Total Nucleic Acid Isolation Kit for FFPE, Thermo Fisher Scientific, Waltham, MA, USA) which allows isolation of RNA including miRs, following the manufacturer's instructions. Extracted RNA was quantified using Nanodrop 1000 (Thermo Fisher Scientific, Waltham, MA, USA).

2.4. MicroRNA profiling

Human miR microfluidic cards, TaqMan Array Human MicroRNA A + B Cards Set v3.0 (Applied Biosystems by Thermo Fisher Scientific, Waltham, MA, USA), containing 754 human miR assays, were used to identify miR-profiles among the healthy arteries. Ten Cards A and 10 Cards B were used for profiling abdominal aorta, carotid and femoral arteries.

RNA was converted to cDNA by priming with a mixture of looped primers and then pre-amplified using the MegaPlex primer pools (Applied Biosystems by Thermo Fisher Scientific, Waltham, MA, USA) according to manufacturer's instructions. The profiling was performed using an Applied Biosystems 7900 H T real-time PCR instrument.

2.5. Validation in single RT-qPCR

Ten ng of healthy arteries tissue RNA were transcribed to cDNA with

Table 1
Numbers of artery biopsies and sample size. Each sample was obtained from a different individual.

Human biopsies	Group	Sex	Age	Obtained from	Pathology or cause of death	Surgical procedure
Carotid artery 1	Normal	Female	46	Organ donor	Cerebral hemorrhage	Resection
Carotid artery 2	Normal	Male	38	Organ donor	Traumatic injury	Resection
Carotid artery 3	Atherosclerotic	Male	74	Patient	Atherosclerotic plaque	Endarterectomy
Carotid artery 4	Atherosclerotic	Female	47	Patient	Atherosclerotic plaque	Endarterectomy
Carotid artery 5	Atherosclerotic	Male	47	Patient	Atherosclerotic plaque	Endarterectomy
Carotid artery 6	Atherosclerotic	Male	47	Patient	Atherosclerotic plaque	Endarterectomy
Abdominal Aorta 1	Normal	Female	23	Organ donor	Cardiovascular disease	Resection
Abdominal Aorta 2	Normal	Female	27	Organ donor	Traumatic injury	Resection
Abdominal Aorta 3	Normal	Male	31	Organ donor	Electrocution	Resection
Abdominal Aorta 4	Normal	Male	42	Organ donor	Traumatic injury	Resection
Abdominal Aorta 5	Atherosclerotic	Female	63	Patient	Cerebral hemorrhage	Endarterectomy
Abdominal Aorta 6	Atherosclerotic	Male	59	Patient	Cerebral hemorrhage	Endarterectomy
Femoral artery 1	Normal	Female	27	Organ donor	Traumatic injury	Resection
Femoral artery 2	Normal	Female	47	Organ donor	Traumatic injury	Resection
Femoral artery 3	Normal	Male	35	Organ donor	Traumatic injury	Resection
Femoral artery 4	Normal	Male	31	Organ donor	Cerebral hemorrhage	Resection
Femoral artery 5	Atherosclerotic	Female	54	Patient	Atherosclerotic plaque	Endarterectomy
Femoral artery 6	Atherosclerotic	Male	56	Patient	Atherosclerotic plaque	Endarterectomy
Femoral artery 7	Atherosclerotic	Male	55	Patient	Atherosclerotic plaque	Endarterectomy
Femoral artery 8	Atherosclerotic	Male	55	Patient	Atherosclerotic plaque	Endarterectomy

the TaqMan MicroRNA Reverse Transcription Kit (Applied Biosystems, by Thermo Fisher Scientific, Waltham, MA, USA) and the real-time quantitative PCR (RT-qPCR) was subsequently performed with TaqMan MicroRNA Assays. The RNU48 value of each artery sample was used for normalization, obtaining ΔCt values, and relative expressions were calculated by using the $2^{-\Delta Ct}$ method. Confirmed miRs were then analyzed by RT-qPCR in atherosclerotic arteries under the same standardized procedures.

2.6. Bioinformatics analyses

Two different bioinformatics analyses were conducted. The first one focused on experimentally validated gene targets and they were obtained from TarBase v.8 database (Karagkouni et al., 2018). Among the miRs' targets, those considered of interest for previous results and their potential role in endothelial to mesenchymal transition (EndMT) and inflammation were selected, *i.e.*, vimentin, E-cadherin and CD44. The second investigation was aimed to identify common pathways *via* Kyoto Encyclopedia of Genes and Genomes (KEGG) with *p*-values <0.05, using mirPath software for DIANA tools (Vlachos et al., 2015).

2.7. Immunohistochemical (IHC) assay

IHC for vimentin (clone V9, prediluted) and E-cadherin (clone 36, prediluted) was automatically performed by means of the automated immunostainer Benchmark® ultra (Ventana Medical Systems, Inc, Roche group, Tucson AZ, USA), following the manufacturer's instructions.

For detection of SLUG and CD44 proteins, manual IHC was performed through non-biotin amplified method (Novolink™ DAB polymer, Leica Microsystems Srl Milan, Italy). Sections (4 μm thick) of formalin-fixed and paraffin-embedded tissues were deparaffinized and rehydrated through a series of graded ethanol and rinsed in distilled water. Endogenous peroxidase activity was blocked in 3% H_2O_2 in absolute methanol for 10 min at room temperature (R.T.); antigen retrieval was performed using citrate buffer (pH 6) in autoclave (120 °C) for 20 min. After cooling, slides were washed with Tris Buffered Saline (TBS), and then incubated with SLUG primary antibody (1:500; Santa Cruz Biotechnology Dallas, Texas USA) and CD44 (1:100; BD Pharmigen San Jose, CA, USA) in a moist chamber at 4 °C overnight. Then, slides were incubated with NovoLink Polymer for 30 min at R.T. and then exposed to the substrate/chromogen 3,3′-diaminobenzidine (DAB) prepared from Novocastra DAB Chromogen and NovoLink DAB buffer. Nuclei were counterstained with Mayer's haematoxylin. Samples were dehydrated, cover slipped and observed under a light microscope using the Image Pro Plus program.

Quantification of IHC stain was performed on digitalized images randomly acquired at 25X magnification, and a minimum of 5 histological sections was examined for each sample, by using Image J software. Results were expressed as percentage of positive areas.

2.8. Statistical analysis

MiRs profiling was normalized using the median of the overall miR expression on each array (ΔCt). Only miRs expressed in all the samples were selected for analyses and Ct values ≤ 30 were established as cut-off. Fold-change ($2^{-\Delta\Delta CT}$) was calculated based on the estimated mean difference between vascular groups. Fold changes (FC) ≥2 and ≤-2 were selected. Statistical analyses for miRs and target data were performed with parametric or not-parametric test by means of IBM SPSS, version 25 (SPSS Inc., USA).

Hierarchical clustering was performed on 29 miRs, being those statistically significant comparing normal arteries (Mann-Whitney and t tests), and squared Euclidian distance with Ward linkage was applied (confirmed also using average linkage).

3. Results

MiR profiling comparisons among normal arteries are shown in Figures S1−3 (abdominal aorta *vs* carotid artery; abdominal aorta *vs* femoral artery; femoral *vs* carotid artery, as average results), where all miRs with FC ≥ 2 and FC ≤-2 are reported. The smaller number of different expressed miRs was found comparing abdominal aorta and carotid artery (25 out of 734 miRs applying FC, Figure S1). Moreover, statistical analysis revealed that only 3 out of 25 miRs displayed statistically significant differences (*p*-value <0.05, miR-139-5p, -216a, -27a-5p) between normal aorta and carotid arteries. Statistical analysis comparing aorta, carotid *vs* femoral arteries, identified a list of 39 and 46 miRs, respectively. Hierarchical clustering, as reported in Figure S4, confirmed the similarity between aorta and carotid miRs profiling. Thus, aiming at increasing the power and grasping the difference with femoral arteries, aorta and carotid data were combined in single group.

A total of 10 miRs were selected for subsequent validation phase. Nine out of 10 miRs were selected for both highest FC and significant *p*-values, *i.e.*, miR-10b, -155-5p, -145-5p, -126-3p, -139-5p, -143-3p, -216a, -27a-5p, -125a-5p. Additionally, miR-21-5p was selected for previous results obtained by our group including a role as InflammamiR (Olivieri et al., 2013). Among the 10 selected miRs, those significant comparing aorta and carotid arteries were also included, *i.e.*, miR-139-5p, -216 a, -27a-5p. However, validation phase performed with a higher resolution technique (RT-qPCR) showed no differences for these miRs. The result confirmed what emerged from the hierarchical clustering analysis (Figure S4) indicating the consistent similarity between aorta and carotid artery in comparison with femoral artery. Overall, 3 out of 10 miRs selected were confirmed to be differentially expressed comparing normal femoral arteries and aorta/carotid, *i.e.*, miR-155-5p; -27a-5p; and -139-5p. These three miRs were also measured in atheromas obtained from the different type of atherosclerotic arteries.

The results are shown in Fig. 1 (panels A–C) where the three selected miRs (miR-155-5p; -27a-5p; and -139-5p) in normal and atherosclerotic conditions of different arteries are reported. MiR-155−5p has higher expression in normal aorta/carotid than femoral arteries, but in atherosclerotic tissue its level increases in pathological femoral artery only. By contrast, miR-139-5p has lower expression in both normal and pathological aorta/carotid arteries, and miR-27a-5p displays opposite expression levels comparing normal arteries with their pathological counterpart.

Target genes of the three selected miRs were considered on the basis of our previous data related to EndMT, *i.e.*, CD44, vimentin and E-cadherin (Valente and Pasquinelli, 2017). Similarly, SLUG was investigated due to its accepted role in EndMT (Ciavarella et al., 2021; Sánchez-Duffhues et al., 2018).

Vimentin expression, a validated target of miR-155-5p, is shown in normal and atheroma conditions of the arteries (Fig. 2). The level of vimentin suggests the proportional presence of cells in the different normal and pathological conditions of arteries, being significantly reduced in atheroma, as expected.

CD44, a validated mRNA-target of both miR-155-5p and miR-27a-5p, is highly expressed as protein in endothelial and inflammatory cells; its expression was significantly higher in atheroma of aorta/carotid *vs* femoral arteries, as reported in Fig. 3 (panel C), while no significant differences were found between normal arteries (data not shown). The differential expression of CD44 in atherosclerotic plaques was found concomitant with the presence of inflammatory cells in carotid and aorta atheroma, as observed in histological imaging (Fig. 3 panels A, B).

E-cadherin, a validated mRNA-target of miR-139-5p, is shown as protein expression in Fig. 4 in both normal and atheroma conditions of different arteries. A higher level of expression was found in normal femoral artery than normal aorta/carotid arteries. An increase of expression levels was found in atherosclerotic aorta/carotid group

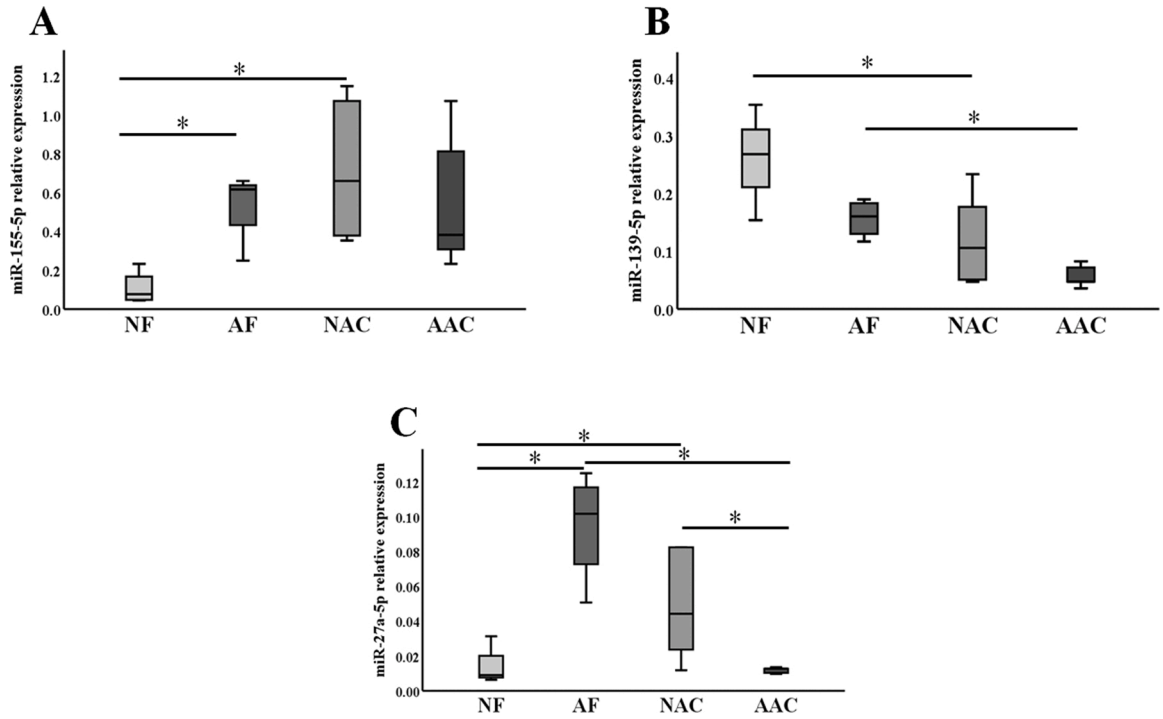

Fig. 1. RT-qPCR analysis of selected miRs in normal and atheroma arteries. Data are shown as box plots representing miR-155-5p (A), miR-139-5p (B) and miR-27a-5p (C) relative expression levels. Data were normalized by RNU48 expression levels. *p*-values were calculated with Mann-Whitney *U* test. Significance was set at **p*-value <0.05.
Abbreviations: NF normal femoral artery; AF atherosclerotic femoral artery; NAC normal abdominal aorta/carotid artery; AAC atherosclerotic abdominal aorta/carotid artery.

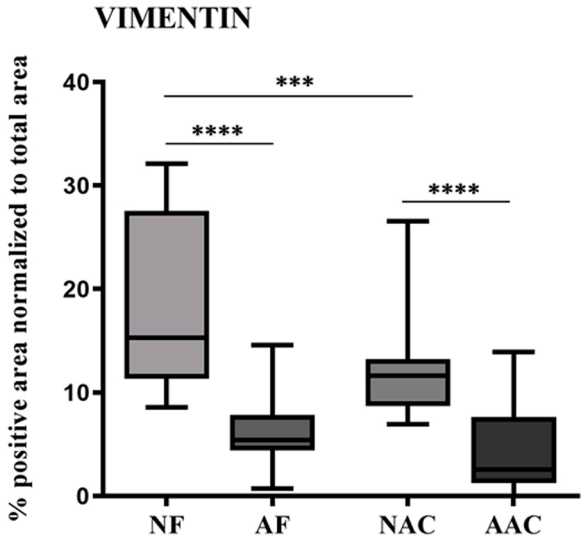

Fig. 2. Vimentin expression decreases in atherosclerotic lesions. Immunohistochemical detection of vimentin expression was quantified by calculating the percentage of positive areas through ImageJ software; data are reported as box plots. Statistical analysis was assessed by one-way Anova. ****p*-value <0.001; *****p*-value <0.0001.
Abbreviations: NF: normal femoral artery; AF: atherosclerotic femoral artery; NAC: normal aorta/carotid artery; AAC: atherosclerotic aorta/carotid artery.

compared to the normal counterpart. By contrast, no significant difference was observed between pathological arteries.

SLUG protein levels are shown in Fig. 5, both in normal and atheroma conditions. SLUG increases in pathological conditions, but it was significantly elevated only in the atheroma of aorta/carotid arteries compared with the normal counterpart. The level of expression was higher in the atheroma of aorta/carotid than femoral arteries.

Table 2 shows the correlation of miR expression with the levels of protein targets inside atheroma from different arteries. No significant correlation was found investigating normal tissues (data not shown).

A second bioinformatic approach, revealed that miR-155-5p with miR-27a-5p, may modulate the TGF-beta signaling (KEGG pathway *p*-value = 4.00E+01), while miR-155-5p and miR-139-5p, may modulated NF-κB signaling (KEGG pathway *p*-value = 9.36E-04). Considering miR-27a-5p and miR-139-5p, among the most significant KEGG pathways Hippo-signaling (*p*-value = 3.07E+00) was identified. No shared pathways were identified considering all three miRs.

4. Discussion

Atherosclerosis can be considered both a tissue-specific and a systemic accelerated aging process associated with inflammaging (Collura et al., 2020; Franceschi et al., 2017, 2007, 2000) and in turn, the aging process may accelerate atherosclerosis when morbidities/comorbidities are present (Franceschi et al., 2018). However, inside this apparent vicious circle, arteriogenesis and artery cell structure play important roles in atheroma development.

In this perspective, the current work draws its inspiration from the necessity of a refined knowledge of human normal arteries considering not only morphology/histopathology, but also molecular expression and epigenetics, often not available in published articles.

MiR-profiling in human normal abdominal aorta, carotid and femoral arteries revealed more similarities between abdominal aorta and carotid arteries than between femoral and the other two arteries. Thus, aiming at identifying the difference in terms of expressed miRs and increasing statistical power, aorta and carotid data were combined and compared with femoral artery. Actually, one limitation of this work is the relatively low number of sampled normal carotid arteries, but the human origin of the tissue samples represents an added value for the

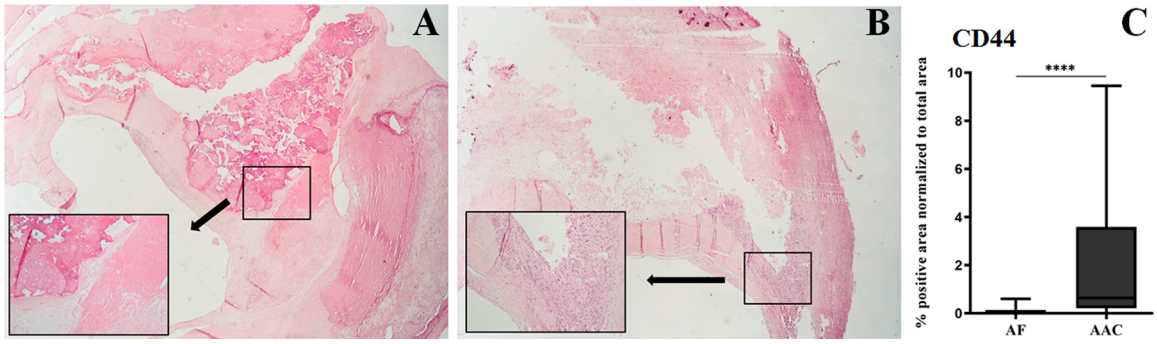

Fig. 3. (A) **A pathological femoral artery**, showing a dense intimal calcium deposit, without significant inflammatory infiltrate. The higher-magnification square on the lower left shows the scarce cellularity of the lesion. (B) **A pathological carotid artery**, with a necrotic-lipidic core and a severe inflammatory infiltrate. The higher-magnification square on the lower left highlights the dense cellularity in the lesion's shoulder, mainly due to a dense macrophagic infiltrate. (C) **CD44 expression**. The different intra-plaque cellularity is reflected by a significantly different CD44 expression (p-value<0.0001). Immunohistochemistry quantification was performed by calculating the percentage of positive areas through ImageJ software; data are reported as box plot. Statistical analysis was assessed by unpaired Student t-test; ****p-value <0.0001.
Abbreviations: AF: atherosclerotic femoral artery; AAC: atherosclerotic aorta/carotid artery.

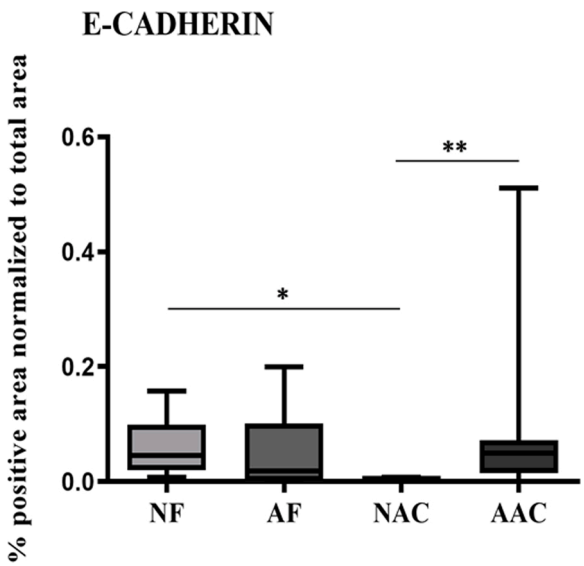

Fig. 4. E-cadherin is differently expressed in normal femoral *vs* aorta/carotid arteries and is increased in atherosclerotic aorta/carotid arteries *vs* normal counterpart. Immunohistochemical detection of E-cadherin expression was quantified by calculating the percentage of positive areas through ImageJ software; data are reported as box plots. Statistical analysis was assessed by unpaired Student t-test; *p-value <0.05 **p-value <0.01.
Abbreviations: NF: normal femoral artery; NAC: normal aorta/carotid artery; AF: atherosclerotic femoral artery; AAC: atherosclerotic aorta/carotid artery.

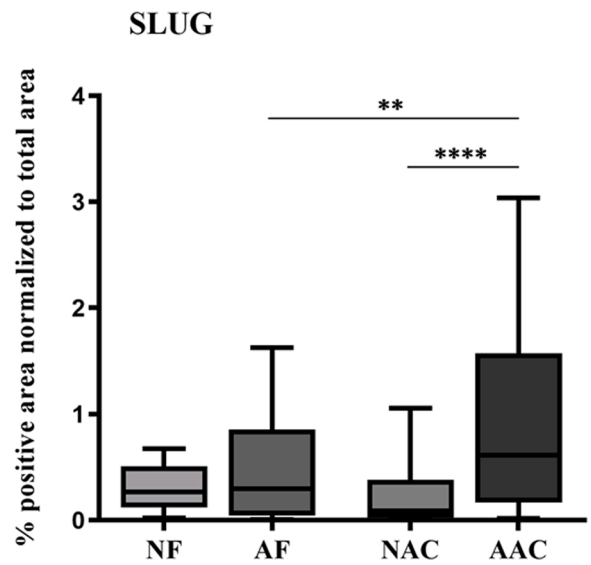

Fig. 5. SLUG expression is increased in atherosclerotic aorta/carotid lesions. Immunohistochemical detection of SLUG expression was quantified by calculating the percentage of positive areas through ImageJ software; data are reported as box plots. Statistical analysis was assessed by one-way Anova. **p-value <0.01; ****p-value <0.0001.
Abbreviations: NF: normal femoral artery; AF: atherosclerotic femoral artery; NAC: normal aorta/carotid artery; AAC: atherosclerotic aorta/carotid artery.

advancement of knowledge. An additional limitation was the relatively low amount of bioptic mRNAs, thus proteins were the targets of miRs to be efficiently investigated.

Among miRs selected for validation, three resulted significantly modified comparing normal arteries, *i.e.*, miR-27a-5p, -139-5p, and -155-5p. In particular, miR-155-5p e miR-27a-5p turned out to be more highly expressed in normal aorta/carotid than femoral arteries, while miR-139-5p showed the opposite direction suggesting a different epigenetic pattern in the normal arteries investigated.

As far as atheroma is concerned, data we obtained from old adults suggest that the three miRs have also relevance in pathological conditions. In fact, femoral atheroma showed an increased miR-155-5p and miR-27a-5p expression when compared with the normal counterpart, thus the level of those miRs become more similar to normal carotid/abdominal aorta arteria.

Table 2
Correlation between miRs expressed in atherosclerotic arteries and selected targets.

Arteries	Correlation between miR and target	r	p-value
Atherosclerotic Femoral	CD44 and miR-27a-5p	0.998	0.040
Atherosclerotic Aorta/ Carotid	Vimentin and miR-155-5p	0.968	0.001
Atherosclerotic Aorta/ Carotid	Vimentin and miR-139-5p	0.843	0.035
Atherosclerotic Aorta/ Carotid	E-cadherin and miR-27a-5p	0.999	<0.001
Atherosclerotic Aorta/ Carotid	E-cadherin and miR-139-5p	0.992	<0.001

Interestingly, miR-155-5p is involved in inflammatory pathway regulation (Olivieri et al., 2013) and seems also to be associated with atherosclerosis (Chen et al., 2019; Fitzsimons et al., 2020). Similarly, miR-27a is able to regulate the inflammatory response of macrophages (Xie et al., 2014). A recent work suggests that miR-27a-5p is involved in the regulation of lymphotoxin beta receptor and nuclear factor-kappa B activation in lipopolysaccharides-stimulated vascular smooth muscle cells (VSCs) (Ling et al., 2020).

Thus, comparing pathological tissues in old adults, femoral atheroma showed higher miR-27a-5p and miR-139-5p expression than carotids/aorta. In this regard, miR-139-5p was found to be involved in plaque formation, and inflammatory response in atherosclerosis animal models (Zheng et al., 2021).

The additional investigation of important targets of the emerged miRs, such as vimentin, CD44 and E-cadherin revealed also positive correlation with some of them, but only in pathological conditions and with differences among arteries. In fact, aorta/carotid had a greater number of correlations than femoral atheroma, suggesting a different epigenetic/expression changes in pathological conditions.

Vimentin displayed an opposite expression pattern when compared to miR-155-5p in normal femoral arteries as expected, but this trend was not found in normal aorta/carotid arteries. These findings suggest different levels of protein regulation in the two artery districts likely including the regulation of other molecular mediators, as also suggested by literature in an *in vitro* model (Wang et al., 2017). In addition, the decrease of cellularity in atheroma leads to a decrease in vimentin level.

SLUG protein also showed an increased expression in atheroma of aorta/carotid arteries, but not in femoral artery. On the contrary, E-cadherin showed a higher expression in normal femoral than aorta/carotid arteries and in atherosclerotic aorta/carotid arteries compared to normal counterpart, thus supporting the hypothesis that aorta/carotid and femoral arteries have different molecular drivers, likely involved in molecular and cellular changes leading to atheroma. Aorta and carotid atheroma may likely develop through an EndMT process (Chen et al., 2020) with strong inflammatory component participation, as also shown in the histopathological analyses that are dominated by the fibro-lipidic inflammatory atheroma histotype. Accordingly, the high levels of miR-155-p and miR-27a-5p in normal aorta/carotid arteries may support the hypothesis of the TGF-beta signaling involvement for EndMT (Chen et al., 2020).

Correlation results between miRs and their protein-targets were largely unexpected, likely due to the protein assessment instead of mRNAs, but highlighting differences among atherosclerotic arteries. Actually, the expression of a target could be modulated by a high number of miRs and other molecular/epigenetic regulators. Thus, not always a direct correlation or anti-correlation between the expression of a miR and its target could be identified, as previously observed (Kangas et al., 2018). Actually, the hemodynamic patterns may prime the gene expression/epigenetics profile of vascular cells in slightly different ways so that arteries react differently to the aging process and cardiovascular risk factors at relatively young ages. This possibility is supported on distinct SMC phenotypes in rat aorta media (Hao et al., 2003) and by the predominance in human atherosclerotic arteries of SMC with synthetic phenotype reminiscent of juvenile muscle cells seen in the course of embryogenesis (Alexander and Owens, 2012). The evolution of the atheroma *in vivo* appears to depend on the relative replicative activity and/or susceptibility to apoptosis of these phenotypes primed by hemodynamic and cardiovascular risk factors (Hao et al., 2003).

Overall, atheroma is a peculiar microenvironment that differently affects various arteries, and the genomic make-up also contributes (Steenman et al., 2018; Sulkava et al., 2017). In particular, bone development-related genes were among those mostly enriched in atherosclerotic and healthy femoral arteries, which are more prone to calcification. These results are also consistent with the present findings. In addition, protein CD44, E-cadherin, vimentin, and SLUG characterize each arteria and each type of cells. In particular, the femoral artery has an unexpected distribution of these markers, both in normal and atheroma conditions, and likely, a distinct pathway of activation in the atheroma condition may be envisaged. In this respect, TGF-beta signaling is one of those involved in EndMT, characterizing aorta/carotid atheroma arteries (Ciavarella et al., 2021; Sánchez-Duffhues et al., 2018). Previously, we studied the characteristics of the SMC, *e.g.*, vascular mesenchymal stromal stem cells (MSC) from different normal human arterial districts and they revealed differences in molecular expressions and functional activities in femoral arteries; in particular, a more mesenchymal fibroblast-like phenotype was observed, likely reflecting a less regenerative potential to vascular injury response (Valente and Pasquinelli, 2017).

In conclusion, the present work improves the knowledge to understand the molecular differences among arteries and in particular, between femoral *vs* aorta/carotid arteries. The various expression of the miRs-27a-5p, -139a-5p, and -155-5p sustains a differential regulation of mRNAs targets/proteins and may activate different signaling along the pathological process, thus conditioning the morphology of atheroma in adult life. Their role in the different arteries may open the way for a specific atheroma treatment *in situ*. In particular, the future use of the miR:mRNA target network at individual level for atherosclerosis can be improved by the study of phenotypes, like the morphology of atheroma with advanced technique (Chu et al., 2021). The associated molecular/epigenetic changes in *ex vivo* experiments by means of artificial intelligence analysis for discovering common epigenetics-phenotype traits will be a challenge for the next generation of the atherosclerosis treatments.

Author contributions

Conceptualization: G.P., M.G., M.C.; Methodology: S.C., C.C., I.M., S. V., F.V., Surgery: *e.g.*, M.A., R.P., M.G.; Writing: G.P., M.C. C.M. S.C.; Supervision: C.F., M.C., G.P. All authors have read and agreed to the published version of the manuscript.

Institutional review board statement

The study was conducted according to the guidelines of the Declaration of Helsinki and approved by Ethics Committee of S. Orsola Hospital (protocol code: 88/2019/Sper/AOUBo).

Funding

This work was supported by the RFO grant to MC and by FONDAZIONE CARISBO to MC with the project n. #**38-** 2019.0538, entitled "Firma molecolare della patologia carotidea: microRNAs circolanti e rischio cerebrovascolare".

Declaration of Competing Interest

The authors declare no conflict of interest.

Appendix A. Supplementary data

Supplementary material related to this article can be found, in the online version, at doi:https://doi.org/10.1016/j.mad.2021.111547.

References

Alexander, M.R., Owens, G.K., 2012. Epigenetic control of smooth muscle cell differentiation and phenotypic switching in vascular development and disease. Annu. Rev. Physiol. 74, 13–40. https://doi.org/10.1146/annurev-physiol-012110-142315.

Chen, L., Zheng, S.-Y., Yang, C.-Q., Ma, B.-M., Jiang, D., 2019. MiR-155-5p inhibits the proliferation and migration of VSMCs and HUVECs in atherosclerosis by targeting AKT1. Eur. Rev. Med. Pharmacol. Sci. 23, 2223–2233. https://doi.org/10.26355/eurrev_201903_17270.

Chen, P.-Y., Schwartz, M.A., Simons, M., 2020. Endothelial-to-mesenchymal transition, vascular inflammation, and atherosclerosis. Front. Cardiovasc. Med. 7, 53. https://doi.org/10.3389/fcvm.2020.00053.

Chu, M., Jia, H., Gutiérrez-Chico, J.L., Maehara, A., Ali, Z.A., Zeng, X., He, L., Zhao, C., Matsumura, M., Wu, P., Zeng, M., Kubo, T., Xu, B., Chen, L., Yu, B., Mintz, G.S., Wijns, W., Holm, N.R., Tu, S., 2021. Automatic characterisation of human atherosclerotic plaque composition from intravascular optical coherence tomography using artificial intelligence. EuroIntervention. https://doi.org/10.4244/EIJ-D-20-01355.

Ciavarella, C., Motta, I., Vasuri, F., Fittipaldi, S., Valente, S., Pollutri, D., Ricci, F., Gargiulo, M., Pasquinelli, G., 2021. Involvement of miR-30a-5p and miR-30d in endothelial to mesenchymal transition and early osteogenic commitment under inflammatory stress in HUVEC. Biomolecules 11. https://doi.org/10.3390/biom11020226.

Collura, S., Morsiani, C., Vacirca, A., Fronterrè, S., Ciavarella, C., Vasuri, F., D'Errico, A., Franceschi, C., Pasquinelli, G., Gargiulo, M., Capri, M., 2020. The carotid plaque as paradigmatic case of site-specific acceleration of aging process: the microRNAs and the inflammaging contribution. Ageing Res. Rev. 61, 101090 https://doi.org/10.1016/j.arr.2020.101090.

Dalager, S., Paaske, W.P., Kristensen, I.B., Laurberg, J.M., Falk, E., 2007. Artery-related differences in atherosclerosis expression: implications for atherogenesis and dynamics in intima-media thickness. Stroke 38, 2698–2705. https://doi.org/10.1161/STROKEAHA.107.486480.

Fitzsimons, S., Oggero, S., Bruen, R., McCarthy, C., Strowitzki, M.J., Mahon, N.G., Ryan, N., Brennan, E.P., Barry, M., Perretti, M., Belton, O., 2020. microRNA-155 is decreased during atherosclerosis regression and is increased in urinary extracellular vesicles during atherosclerosis progression. Front. Immunol. 11, 576516 https://doi.org/10.3389/fimmu.2020.576516.

Franceschi, C., Bonafè, M., Valensin, S., Olivieri, F., De Luca, M., Ottaviani, E., De Benedictis, G., 2000. Inflamm-aging. An evolutionary perspective on immunosenescence. Ann. N. Y. Acad. Sci. 908, 244–254. https://doi.org/10.1111/j.1749-6632.2000.tb06651.x.

Franceschi, C., Capri, M., Monti, D., Giunta, S., Olivieri, F., Sevini, F., Panourgia, M.P., Invidia, L., Celani, L., Scurti, M., Cevenini, E., Castellani, G.C., Salvioli, S., 2007. Inflammaging and anti-inflammaging: A systemic perspective on aging and longevity emerged from studies in humans. Mech. Ageing Dev. 128, 92–105. https://doi.org/10.1016/j.mad.2006.11.016.

Franceschi, C., Garagnani, P., Vitale, G., Capri, M., Salvioli, S., 2017. Inflammaging and 'Garb-aging.'. Trends Endocrinol. Metab. 28, 199–212. https://doi.org/10.1016/j.tem.2016.09.005.

Franceschi, C., Garagnani, P., Morsiani, C., Conte, M., Santoro, A., Grignolio, A., Monti, D., Capri, M., Salvioli, S., 2018. The continuum of aging and age-related diseases: common mechanisms but different rates. Front. Med. (Lausanne) 5. https://doi.org/10.3389/fmed.2018.00061.

Goossens, E.A.C., de Vries, M.R., Simons, K.H., Putter, H., Quax, P.H.A., Nossent, A.Y., 2019. miRMap: profiling 14q32 microRNA expression and DNA methylation throughout the human vasculature. Front. Cardiovasc. Med. 6 https://doi.org/10.3389/fcvm.2019.00113.

Haimovici, H., Maier, N., 1964. Fate of aortic homografts in canine atherosclerosis. 3. Study of fresh abdominal and thoracic aortic implants into thoracic aorta: role of tissue susceptibility in atherogenesis. Arch. Surg. 89, 961–969. https://doi.org/10.1001/archsurg.1964.01320060029006.

Haimovici, H., Maier, N., Strauss, L., 1958. Fate of aortic homografts in experimental canine atherosclerosis; study of fresh thoracic implants into abdominal aorta. AMA Arch. Surg. 76, 282–288. https://doi.org/10.1001/archsurg.1958.01280200104012.

Haimovici, H., Maier, N., Strauss, L., 1959. Fate of aortic homografts in experimental canine atherosclerosis. II. Study of fresh abdominal aortic implants into abdominal aorta. AMA Arch. Surg. 78, 239–245. https://doi.org/10.1001/archsurg.1959.04320020061010.

Hao, H., Gabbiani, G., Bochaton-Piallat, M.-L., 2003. Arterial smooth muscle cell heterogeneity: implications for atherosclerosis and restenosis development. Arterioscler. Thromb. Vasc. Biol. 23, 1510–1520. https://doi.org/10.1161/01.ATV.0000090130.85752.ED.

Herisson, F., Heymann, M.-F., Chétiveaux, M., Charrier, C., Battaglia, S., Pilet, P., Rouillon, T., Krempf, M., Lemarchand, P., Heymann, D., Gouëffic, Y., 2011. Carotid and femoral atherosclerotic plaques show different morphology. Atherosclerosis 216, 348–354. https://doi.org/10.1016/j.atherosclerosis.2011.02.004.

Jiang, X., Rowitch, D.H., Soriano, P., McMahon, A.P., Sucov, H.M., 2000. Fate of the mammalian cardiac neural crest. Development 127, 1607–1616.

Kangas, R., Morsiani, C., Pizza, G., Lanzarini, C., Aukee, P., Kaprio, J., Sipilä, S., Franceschi, C., Kovanen, V., Laakkonen, E.K., Capri, M., 2018. Menopause and adipose tissue: miR-19a-3p is sensitive to hormonal replacement. Oncotarget 9, 2279–2294. https://doi.org/10.18632/oncotarget.23406.

Karagkouni, D., Paraskevopoulou, M.D., Chatzopoulos, S., Vlachos, I.S., Tastsoglou, S., Kanellos, I., Papadimitriou, D., Kavakiotis, I., Maniou, S., Skoufos, G., Vergoulis, T., Dalamagas, T., Hatzigeorgiou, A.G., 2018. DIANA-TarBase v8: a decade-long collection of experimentally supported miRNA-gene interactions. Nucleic Acids Res. 46, D239–D245. https://doi.org/10.1093/nar/gkx1141.

Libby, P., Buring, J.E., Badimon, L., Hansson, G.K., Deanfield, J., Bittencourt, M.S., Tokgözoğlu, L., Lewis, E.F., 2019. Atherosclerosis. Nat. Rev. Dis. Primers 5, 1–18. https://doi.org/10.1038/s41572-019-0106-z.

Ling, X., Wen, M., Xiao, Z., Luo, Z., Zhuang, J., Li, Q., Du, S., Zheng, S., Zhu, P., 2020. Lymphotoxin beta receptor is associated with regulation of microRNAs expression and nuclear factor-kappa B activation in lipopolysaccharides (LPS)-stimulated vascular smooth muscle cells. Ann. Palliat. Med. 9, 805–815. https://doi.org/10.21037/apm.2020.03.20.

Olivieri, F., Rippo, M.R., Monsurrò, V., Salvioli, S., Capri, M., Procopio, A.D., Franceschi, C., 2013. MicroRNAs linking inflamm-aging, cellular senescence and cancer. Ageing Res. Rev. 12, 1056–1068. https://doi.org/10.1016/j.arr.2013.05.001.

Pouget, C., Gautier, R., Teillet, M.-A., Jaffredo, T., 2006. Somite-derived cells replace ventral aortic hemangioblasts and provide aortic smooth muscle cells of the trunk. Development 133, 1013–1022. https://doi.org/10.1242/dev.02269.

Rea, I.M., Gibson, D.S., McGilligan, V., McNerlan, S.E., Alexander, H.D., Ross, O.A., 2018. Age and age-related diseases: role of inflammation triggers and cytokines. Front. Immunol. 9 https://doi.org/10.3389/fimmu.2018.00586.

Sánchez-Duffhues, G., García de Vinuesa, A., Ten Dijke, P., 2018. Endothelial-to-mesenchymal transition in cardiovascular diseases: developmental signaling pathways gone awry. Dev. Dyn. 247, 492–508. https://doi.org/10.1002/dvdy.24589.

Sigala, F., Oikonomou, E., Antonopoulos, A.S., Galyfos, G., Tousoulis, D., 2018. Coronary versus carotid artery plaques. Similarities and differences regarding biomarkers morphology and prognosis. Curr. Opin. Pharmacol. 39, 9–18. https://doi.org/10.1016/j.coph.2017.11.010.

Steenman, M., Espitia, O., Maurel, B., Guyomarch, B., Heymann, M.-F., Pistorius, M.-A., Ory, B., Heymann, D., Houlgatte, R., Gouëffic, Y., Quillard, T., 2018. Identification of genomic differences among peripheral arterial beds in atherosclerotic and healthy arteries. Sci. Rep. 8, 3940. https://doi.org/10.1038/s41598-018-22292-y.

Sulkava, M., Raitoharju, E., Levula, M., Seppälä, I., Lyytikäinen, L.-P., Mennander, A., Järvinen, O., Zeitlin, R., Salenius, J.-P., Illig, T., Klopp, N., Mononen, N., Laaksonen, R., Kähönen, M., Oksala, N., Lehtimäki, T., 2017. Differentially expressed genes and canonical pathway expression in human atherosclerotic plaques - Tampere Vascular Study. Sci. Rep. 7, 41483. https://doi.org/10.1038/srep41483.

Tzoulaki, I., Castagné, R., Boulangé, C.L., Karaman, I., Chekmeneva, E., Evangelou, E., Ebbels, T.M.D., Kaluarachchi, M.R., Chadeau-Hyam, M., Mosen, D., Dehghan, A., Moayyeri, A., Ferreira, D.L.S., Guo, X., Rotter, J.I., Taylor, K.D., Kavousi, M., de Vries, P.S., Lehne, B., Loh, M., Hofman, A., Nicholson, J.K., Chambers, J., Gieger, C., Holmes, E., Tracy, R., Kooner, J., Greenland, P., Franco, O.H., Herrington, D., Lindon, J.C., Elliott, P., 2019. Serum metabolic signatures of coronary and carotid atherosclerosis and subsequent cardiovascular disease. Eur. Heart J. 40, 2883–2896. https://doi.org/10.1093/eurheartj/ehz235.

Valente, S., Pasquinelli, G., 2017. Phenotypic and functional mapping of mesenchymal stem cells harvested from different portions of the human arterial tree. Mesenchymal Stem Cells - Isolation, Characterization and Applications. https://doi.org/10.5772/intechopen.68427.

Vasuri, F., Fittipaldi, S., Pacilli, A., Buzzi, M., Pasquinelli, G., 2016. The incidence and morphology of Monckeberg's medial calcification in banked vascular segments from a monocentric donor population. Cell Tissue Bank. 17, 219–223. https://doi.org/10.1007/s10561-016-9543-z.

Vasuri, F., Ciavarella, C., Fittipaldi, S., Pini, R., Vacirca, A., Gargiulo, M., Faggioli, G., Pasquinelli, G., 2020. Different histological types of active intraplaque calcification underlie alternative miRNA-mRNA axes in carotid atherosclerotic disease. Virchows Arch. 476, 307–316. https://doi.org/10.1007/s00428-019-02659-w.

Verzi, M.P., McCulley, D.J., De Val, S., Dodou, E., Black, B.L., 2005. The right ventricle, outflow tract, and ventricular septum comprise a restricted expression domain within the secondary/anterior heart field. Dev. Biol. 287, 134–145. https://doi.org/10.1016/j.ydbio.2005.08.041.

Vlachos, I.S., Zagganas, K., Paraskevopoulou, M.D., Georgakilas, G., Karagkouni, D., Vergoulis, T., Dalamagas, T., Hatzigeorgiou, A.G., 2015. DIANA-miRPath v3.0: deciphering microRNA function with experimental support. Nucleic Acids Res. 43, W460–W466. https://doi.org/10.1093/nar/gkv403.

Wang, J., He, W., Xu, X., Guo, L., Zhang, Y., Han, S., Shen, D., 2017. The mechanism of TGF-β/miR-155/c-Ski regulates endothelial–mesenchymal transition in human coronary artery endothelial cells. Biosci. Rep. 37 https://doi.org/10.1042/BSR20160603. BSR20160603.

Wasteson, P., Johansson, B.R., Jukkola, T., Breuer, S., Akyürek, L.M., Partanen, J., Lindahl, P., 2008. Developmental origin of smooth muscle cells in the descending aorta in mice. Development 135, 1823–1832. https://doi.org/10.1242/dev.020958.

Wiegreffe, C., Christ, B., Huang, R., Scaal, M., 2009. Remodeling of aortic smooth muscle during avian embryonic development. Dev. Dyn. 238, 624–631. https://doi.org/10.1002/dvdy.21888.

Xie, N., Cui, H., Banerjee, S., Tan, Z., Salomao, R., Fu, M., Abraham, E., Thannickal, V.J., Liu, G., 2014. miR-27a regulates inflammatory response of macrophages by targeting IL-10. J. Immunol. 193, 327–334. https://doi.org/10.4049/jimmunol.1400203.

Zheng, X., Zhao, X., Han, Z., Chen, K., 2021. Enhancer of zeste homolog 2 participates in the process of atherosclerosis by modulating microRNA-139-5p methylation and signal transducer and activator of transcription 1 expression. IUBMB Life 73, 238–251. https://doi.org/10.1002/iub.2423.